Journal of Tropical Resources and Sustainable Science
Website : http://journal.umk.edu.my/index.php/jtrss/
eISSN : 2462-2389
Vol: SI Issue 1, 2025, 153-161
DOI: https://doi.org/10.47253/jtrss.v13i3.2012

RESEARCH ARTICLE

Geophysical investigation of subsurface structure using electrical resistivity imaging (ERI) and induced polarization (IP) methods in metaigneous terrains of Jeli, Kelantan, Malaysia

Nur Farhana Ab Malik[1], Hamzah Hussin[*2,3], Abdul Hafidz Yusoff[1,3], Noor Fazliani Shoparwe[1,3] and Che Muhammad Hazwan Che Ismail[3]

[1]Faculty of Bioengineering and Technology, Universiti Malaysia Kelantan, 17600 Jeli, Kelantan, Malaysia.
[2]Faculty of Earth Science, Universiti Malaysia Kelantan, 17600 Jeli, Kelantan, Malaysia.
[3]Gold, Rare Earth and Materials Technopreneurship Centre (GREAT), Universiti Malaysia Kelantan, 17600 Jeli, Kelantan, Malaysia.

ARTICLE HISTORY
Received : 5 August 2025
Accepted : 25 October 2025
Online : 31 December 2025

KEYWORDS
Geophysical investigation,
Electrical Resistivity Imaging,
Induced Polarization,
metaigneous rock,
Central Belt,
subsurface structure

☒ * **CORRESPONDING AUTHOR**
Hamzah Hussin
Gold, Rare Earth and Materials Technopreneurship Centre (GREAT), Universiti Malaysia Kelantan, 17600 Jeli, Kelantan, Malaysia
Email: hamzah.h@umk.edu.my

ABSTRACT

This study presents a geophysical investigation of subsurface structures within the metaigneous terrains of selected area located in Jeli, Kelantan using integrated Electrical Resistivity Imaging (ERI) and Induced Polarization (IP) methods. The study area is located within Universiti Malaysia Kelantan Jeli Campus, Jeli District, Kelantan, and lies within the Central Belt of Peninsular Malaysia. Geological mapping at this area revealed the presence of metaigneous rocks, offering critical insights into the lithological distribution and structural deformation history of the region. Geophysical surveys along selected profiles delineated variations in resistivity and chargeability, identifying key features such as fractured zones, weathered layers, and compact bedrock. High resistivity and moderate-to-high chargeability values correspond to intact metaigneous rock bodies, while lower values indicate weathered or altered zones. The integration of ERI and IP data with surface geological observations provides a comprehensive model of the subsurface, offering insights valuable for Rare Earth Element (REE) mineral exploration.

1. INTRODUCTION

Effective management and sustainable Rare Earth Element (REE) mineral exploration requires a profound understanding of subsurface geological conditions. In regions characterized by complex geological setting, such as those involving significant magmatism and metamorphism, the subsurface can exhibit highly heterogeneous properties that are challenging to characterize solely through surface observations or sparse borehole data Geophysical methods, by offering non-invasive means to probe the Earth's interior and derive its physical properties, have emerged as indispensable tools for geological investigations (Adeniran et al., 2024; Briški et al., 2020; Hussain et al., 2022; Vann et al., 2020; Soupios et al., 2007; Ogungbade et al., 2021; Satir et al., 2021). Similar approaches integrating geospatial mapping with geophysical surveys have also been applied in landslide and terrain susceptibility assessments, further demonstrating their versatility (Badavath & Sahoo, 2025). Among the diverse array of geophysical techniques, Electrical Resistivity Imaging (ERI) and Induced Polarization (IP) stand out for their particular efficacy in delineating lithological variations, mapping groundwater pathways, identifying zones of weathering and fracturing, and detecting various subsurface anomalies that impact environmental applications (Zaid et al., 2023; Martorana & Capizzi, 2023; Vann et al., 2020).

Peninsular Malaysia, particularly its Central Belt, represents a geologically complex and highly prospective region. Its geological evolution is marked by protracted periods of tectonic activity, extensive magmatic intrusions that formed granitic batholiths, and subsequent regional metamorphic events spanning the Paleozoic to Mesozoic eras (Zaid et al., 2023; Martorana & Capizzi, 2023). This intricate history has resulted in a diverse suite of rock types, including metamorphic rocks derived from pre-existing igneous protoliths, known as metaigneous rocks. These rocks, often forming the bedrock in hilly terrains, are subjected to intense tropical weathering processes, leading to the development of deep saprolite profiles, fractured zones, and complex

hydrogeological regimes (Girard et al., 2020; Briški et al., 2020; Rusydy et al., 2021; KC et al., 2025; Sulaiman et al., 2022).

ERI measures the apparent resistivity of the subsurface by injecting controlled electric currents into the ground and measuring the resulting potential differences (Zaid et al., 2023; Martorana & Capizzi, 2023; Alam & Dick, 2024; Fox, R. C., 1979). Resistivity is an intrinsic property of earth materials that is highly sensitive to parameters such as lithology, porosity, water saturation, temperature, and the presence of dissolved ions or clay minerals (Alam & Dick, 2024; Vann et al., 2020). For instance, fresh, dry crystalline rocks exhibit high resistivity, while water-saturated, porous, or clay-rich formations tend to show low resistivity. IP is a complementary geophysical method that measures the subsurface's ability to store electrical charge temporarily in response to an applied current (Alam & Dick, 2024; Martorana & Capizzi, 2023). This phenomenon, known as chargeability, is primarily caused by electrochemical interactions at mineral-water interfaces and is particularly sensitive to the presence of metallic or clay minerals as well as the texture of the pore network within the rock. Thus, by integrating ERI and IP data, a more unambiguous interpretation of subsurface conditions is possible, as different materials may exhibit similar resistivity values but distinct chargeability responses, reducing interpretational ambiguities (Zaid et al., 2023; Martorana & Capizzi, 2023). For example, a low resistivity zone could represent either a clay-rich layer or a highly porous, water-saturated sand layer; however, if the low resistivity zone also exhibits high chargeability, it would strongly suggest a clay-rich or disseminated sulfide-bearing environment rather than clean sand. The effectiveness of ERI can be influenced by factors like salinity, which can reduce resistivity contrast (Adeniran et al., 2024).

Recent advances in near-surface geophysics have shown that electrical methods are particularly effective for subsurface mapping in tropical and crystalline rock terrains. ERI has been extensively applied to estimate the thickness of overburden and regolith, providing quantitative constraints on the depth to bedrock and the lateral variability of weathering intensity (Abidin et al., 2015; Dahlin, 2001; Loke & Barker, 1996). Such approaches are indispensable for delineating different weathering grades, ranging from residual soils to saprolite and fresh bedrock, which are critical for both engineering applications and mineral exploration (Metwaly et al., 2012; Perrone et al., 2014). Integrated ERI and IP studies have also proven helpful in identifying clay-enriched horizons and fractured zones that control groundwater flow and geochemical mobilization in deeply weathered terrains (Uhlemann et al., 2017; Chambers et al., 2014). In addition, the application of geoelectrical techniques for REE exploration in weathered granites has recently gained attention, where ERI is combined with geochemical methods to assess REE-enriched clay horizons (Ogungbade et al., 2021). Collectively, these studies highlight the value of ERI and IP as non-invasive approaches for subsurface characterization, offering insights that complement geological mapping and limited borehole information.

The current study focuses on a geophysical investigation of the hill situated directly in front of the GREAT UMK laboratory at UMK Jeli. The primary objective is to evaluate the critical insights into the weathering profile of the study area. This will be achieved by deploying integrated ERI and IP geophysical surveys along selected profiles. The specific aims include delineating variations in subsurface resistivity and chargeability; identifying subsurface features such as fractured zones, varying degrees of weathered layers, and the extent of compact bedrock; and constructing a comprehensive subsurface model that integrates geophysical findings with surface geological observations. The findings are expected to contribute significantly to the understanding of subsurface conditions in similar metaigneous terrains within tropical environments within the scope of REE exploration.

2. GEOLOGICAL SETTING OF JELI

The Jeli District is strategically located within the geological province known as the Central Belt of Peninsular Malaysia. This belt, trending approximately north-south, forms the backbone of the peninsula and is flanked by the Western Belt (dominated by tin-bearing granites and Paleozoic sedimentary rocks) and the Eastern Belt (characterized by volcanic and sedimentary rocks, and Permo-Triassic granitoids) (Zaid et al., 2023; Martorana & Capizzi, 2023). The Central Belt itself is a mosaic of lithologies, reflecting a complex and poly-deformed history that spans from the Paleozoic to the Mesozoic eras.

The geological evolution of the Central Belt is intricately linked to multiple episodes of subduction, magmatism, and regional metamorphism. During the Permian and Triassic periods, the region experienced intense magmatic arc activity, resulting in the emplacement of voluminous granitic intrusions and the extrusion of associated volcanic rocks. These igneous bodies, along with pre-existing sedimentary sequences (such as argillaceous and arenaceous rocks), were subsequently subjected to significant regional metamorphism during various orogenic events. The resultant metaigneous rocks at UMK Jeli are primarily believed to be meta-granitoids or similar igneous protoliths that have undergone varying degrees of recrystallization and structural

modification due to elevated pressure and temperature conditions (Rusydy et al., 2021; KC et al., 2025).

In tropical environments like Malaysia, the bedrock, including metaigneous rocks, undergoes profound chemical and physical weathering processes due to high temperatures and abundant rainfall (Rusydy et al., 2021; Metwaly et al., 2012; Perrone et al., 2014; Girard et al., 2020; Briški et al., 2020). This typically leads to the formation of a thick regolith profile, which can comprise an upper layer of residual soil, followed by saprolite (weathered rock retaining original rock fabric), and finally grading into fresh bedrock (Rusydy et al., 2021; KC et al., 2025). The depth to fresh bedrock can vary significantly, ranging from a few meters to tens of meters, depending on the rock type, structural discontinuities (e.g., fractures, faults), and local hydrological conditions. Fractured zones, often inherited from regional tectonic stresses or developed through stress relief and weathering, are critical features within these rock masses. They act as pathways for groundwater flow, accelerating weathering processes and significantly influencing the stability of slopes (Girard et al., 2020; Briški et al., 2020). Furthermore, the presence of specific minerals, such as disseminated sulfides (common in some granitic intrusions) or secondary clay minerals formed during weathering, can significantly impact the electrical properties of the rock, making IP a beneficial technique for their detection and characterization (Alam & Dick, 2024).

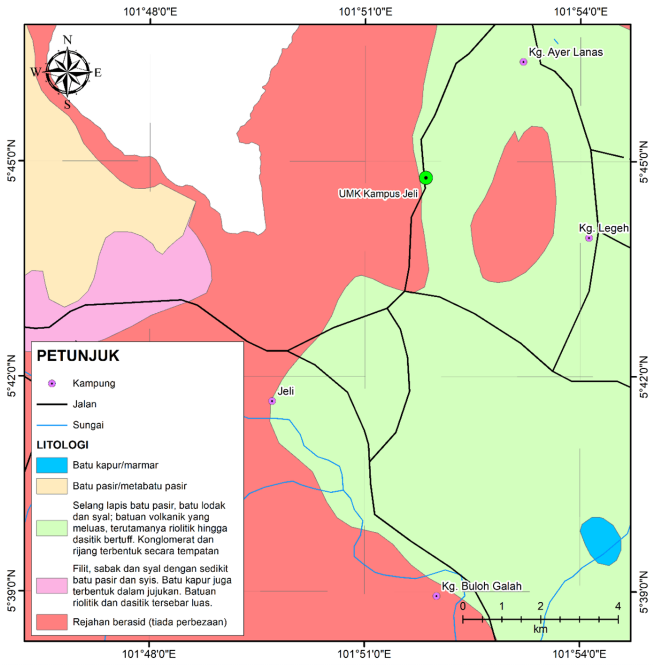

Figure 1: Geological map of the study area, Jeli District, Kelantan.

3. MATERIALS AND METHODS

To achieve the research objectives, a systematic methodology encompassing site selection, deployment of geophysical equipment, data acquisition, and data processing and interpretation was adopted. The approach prioritized the integration of ERI and IP data to leverage the complementary strengths of both techniques.

3.1. Study area

The geophysical investigation was meticulously conducted on the prominent hill within the Universiti Malaysia Kelantan (UMK) Jeli campus. This location was chosen due to its accessibility, known geological context of metaigneous rocks, and its potential for REE study. The study site is characterized by an undulating and moderately steep topography (Figure 2). Elevations within the survey area range approximately from 55 meters to 69 meters above mean sea level (Table 1). The general land cover is dense tropical vegetation, typical of the region, which influences surface drainage and infiltration patterns. The specific geographical coordinates encompassing the survey area extend approximately from 101°52'2 “E to 101°52'6 “E longitude and 5°44'42 “N to 5°44'48 “N latitude.

Figure 2: Topographic map and geophysical survey layout of the study area, Jeli District, Kelantan.

3.2. Geophysical equipment and survey design

The core of the geophysical investigation relied on an advanced ABEM Terrameter LS system, a highly versatile multi-channel resistivity and IP instrument known for its robustness and accuracy in various geological and engineering applications. This instrument is capable of automatic data acquisition for both ERI and IP measurements.

The survey was conducted along four lines, consisting of two parallel lines trending NW-SE and two parallel lines trending NE-SW. These survey lines were systematically established across the study area to ensure comprehensive spatial coverage and to provide cross-sectional views of the subsurface in different orientations relative to the hill's topography (Figure 1). Each survey line

was designed to be 160 meters in length, accommodating 41 stainless steel electrodes. A consistent electrode spacing of 4 meters was maintained for all profiles. The electrode numbering and their precise elevation points were recorded during the field survey, which is crucial for accurate topographic correction during geophysical data processing (Fox, 1979).

Table 1: Electrode elevation data for ERI survey lines at the study area, Jeli District, Kelantan.

Electrode Spacing	Line 1 Elevation (m)	Line 2 Elevation (m)	Line 3 Elevation (m)	Line 4 Elevation (m)
0	57	57	55.5	55
4	58	57	56	55.5
8	58.5	57	56.5	56.5
12	60	57	56.5	57.5
16	62	57	56.5	60.5
20	64.5	57.5	56.5	61.5
24	66.5	61	56.5	64
28	67	61.5	56.5	66
32	68	62	60.5	66.5
36	68.5	62	63	67.5
40	69	61.5	65.5	67.5
44	69	61	66.5	68
48	69.5	61	67.5	68.5
52	69	61	68	68.5
56	69	61.5	68.5	68.5
60	68.5	62	68.5	68.5
64	68	62.5	68.5	68.5
68	67.5	63	68.8	68.5
72	66.5	64	69	68.5
76	66	64.5	69	68.5
80	65.5	65	69	68.5
84	65	66	69	68.5
88	64	66.5	69	67.5
92	63	66.5	69	67
96	62.5	66.5	69	66
100	61	66.5	69	65
104	60	66.5	69	63.5
108	59.5	66.5	69	62
112	59.5	66.5	69	61
116	59	66.5	69	60.5
120	58.5	66.5	69	59.5
124	58	67	69	58.5
128	58	67	68	57.5
132	58	64	66	58
136	57.5	64	64.5	58.5
140	57.5	64	64	58.5
144	57.5	64	64	58.5
148	57	64	64	58.5
152	57	64	64	58.5
156	57	64	64	58.5
160	57	64	64	56.5

The Schlumberger array configuration was selected for data acquisition. This array is particularly well-suited for detailed 2D imaging surveys due to its relatively good lateral resolution and deeper penetration capabilities compared to some other arrays like Wenner or Schlumberger, especially when investigating vertical or steeply dipping structures such as fractured zones (Zaid et al., 2023; Martorana & Capizzi, 2023; Alam & Dick, 2024; Fox, 1979).

3.3. Data acquisition procedure

During the field acquisition phase, a sequential measurement approach was employed for each of the four lines. The ABEM Terrameter LS automatically sequences through various electrode combinations as defined by the chosen array and measurement protocol. For each measurement point, a stable direct current (DC) was injected into the ground through a pair of current electrodes (A and B). The resulting potential difference (voltage) was simultaneously measured across a pair of potential electrodes (M and N), providing the apparent resistivity data. Concurrently, for IP measurements, the current injection was periodically interrupted, and the decay of the secondary voltage (chargeability) after current shut-off was recorded. This typically involves measuring the time-domain decay curve, from which a representative chargeability value (e.g., in milliseconds, msec) is extracted. Multiple cycles of current on/off were performed and stacked to improve the signal-to-noise ratio. Similar integrated approaches, combining geophysical techniques with remote sensing and numerical modeling, have been employed in slope hazard and landslide assessments (Tandon et al., 2022). The system systematically explored all possible electrode combinations to build a comprehensive dataset for the 2D pseudo-section. Care was taken to ensure good electrical contact between the electrodes and the ground by moistening the soil around the electrodes as necessary, thereby minimizing contact resistance and ensuring data quality.

3.4. Data processing and inversion

The raw apparent resistivity and chargeability data acquired in the field were imported into a specialized 2D resistivity and IP inversion software, typically Res2DINV (Zaid et al., 2023; Martorana & Capizzi, 2023; Vann et al., 2020). The inversion process is crucial for transforming the apparent resistivity and chargeability values, which are influenced by the array geometry and subsurface heterogeneity, into true subsurface resistivity and chargeability models.

The inversion algorithm employed in Res2DINV is based on a robust least-squares approach (Loke & Barker, 1996; Dahlin & Zhou, 2004; Abidin et al., 2015; Zaid et al., 2023; Martorana & Capizzi, 2023). This algorithm works by constructing an initial subsurface model, often a homogeneous half-space, then calculating the apparent resistivity/chargeability responses for this model. It then compares the calculated responses with the actual observed field data and adjusts the subsurface model iteratively to minimize the difference (error) between the calculated and

observed data. Topographic corrections are applied during the inversion process by incorporating the collected electrode elevation data into the model geometry. This is particularly critical in hilly terrains like the study area, as it prevents artifacts in the inverted sections from being mistaken for geological features (Fox, R. C., 1979). The inversion process typically continues until a satisfactory Root Mean Square (RMS) error or absolute error is achieved. For all four profiles in this study, the inversion process successfully converged after several iterations; notably, the absolute errors consistently remained remarkably low, typically ranging from 1.0% to 2.0%. These low error values indicate a good fit between the measured field data and the calculated responses from the final inverted models, lending high confidence to the generated tomograms.

3.5. Data interpretation methodology

The interpretation of the inverted 2D resistivity and chargeability tomograms was carried out by integrating geophysical principles with the known geological context of metaigneous rocks in a tropical weathering environment. The fundamental premise is that variations in electrical properties directly correlate with changes in subsurface lithology, degree of weathering, fluid content, and structural features.

The interpretation of the inverted 2D resistivity and chargeability tomograms was carried out by integrating geophysical principles with the known geological context of metaigneous rocks in a tropical weathering environment. The fundamental premise is that variations in electrical properties directly correlate with changes in subsurface lithology, degree of weathering, fluid content, and structural features.

Chargeability Interpretation Principles: High chargeability, typically exceeding ten milliseconds, can indicate the presence of disseminated metallic minerals (e.g., sulfides, graphite), significant amounts of clay minerals (due to their surface electrochemical properties), or highly porous media saturated with conductive fluids, especially in a fine-grained matrix (Alam & Dick, 2024). In weathered granitic terrains, high chargeability often points to the accumulation of secondary clay minerals or possibly relict disseminated sulfides (Alam & Dick, 2024). Moderate chargeability, ranging from four to ten milliseconds, often corresponds to sandy and silty soils or moderately weathered bedrock with some clay content. Low chargeability, typically below four milliseconds, is generally indicative of resistive, unfractured, and dry materials such as fresh crystalline bedrock, or clean, coarse-grained sediments (e.g., gravels, coarse sands) with low clay content.

Integrated Interpretation (ERI + IP): The strength of using both ERI and IP lies in their complementary nature. For instance, a zone of low resistivity and high chargeability is often diagnostic of a clay-rich layer, highly weathered and saturated rock, or mineralized zones. This signature is critical for identifying potential groundwater aquifers in saprolitic zones or highly fractured rock (Martorana & Capizzi, 2023). A zone of high resistivity and low chargeability typically represents dry, competent bedrock or immaculate, dry granular material. A zone of high resistivity and high chargeability could indicate dry, disseminated mineralization or highly resistive rock with significant surface polarization effects, such as highly fractured dry rock with a clay coating. A zone of low resistivity and low chargeability may suggest highly saline groundwater in a porous medium, or a highly permeable zone with rapid fluid movement that prevents charge build-up. By meticulously analyzing these combined responses, geological features such as different weathering grades (e.g., dry versus saturated granitic soil), potential groundwater aquifers, and inferred fractured zones can be identified and mapped with greater confidence in the subsurface. The direct annotations provided within the inverted sections (e.g., "Highly saturated granitic soil (river infiltration)", "Possible groundwater aquifer") were also critically evaluated and integrated into the interpretation process.

4. RESULT AND DISCUSSION

The processed 2D inverted resistivity and chargeability tomograms for all four survey lines provide detailed cross-sectional views of the subsurface electrical properties, allowing for the identification and interpretation of various geological and hydrogeological features. Each tomogram is presented with topographical correction, ensuring that the features are accurately positioned relative to the varying surface elevation.

4.1 Line 1: subsurface characteristics

The resistivity and chargeability tomograms along Line 1 (Figure 3) reveal distinct subsurface characteristics, both in the shallow and deeper regions. The uppermost horizon, extending from the surface down to approximately five meters, is dominated by relatively high resistivity values ranging from about 500 to more than 2000 Ω·m. Such responses are characteristic of dry, compacted granitic soil, indicating limited moisture infiltration and a dense, well-compacted overburden. The corresponding chargeability values in this near-surface interval remain comparatively subdued, typically fluctuating between 0 and 10 milliseconds. These values are most consistent with sandy to silty granitic regolith containing only minor clay fractions. In contrast, the

deeper portions of the section, particularly in the western segment, display a pronounced anomaly characterized by low resistivity (<100 Ω·m) coupled with elevated chargeability, exceeding 10 milliseconds and in some places rising above 30 milliseconds. The spatial coincidence of these signatures strongly supports the interpretation of a weathered and clay-rich saturated zone, most likely functioning as a shallow unconfined aquifer within decomposed granitic material.

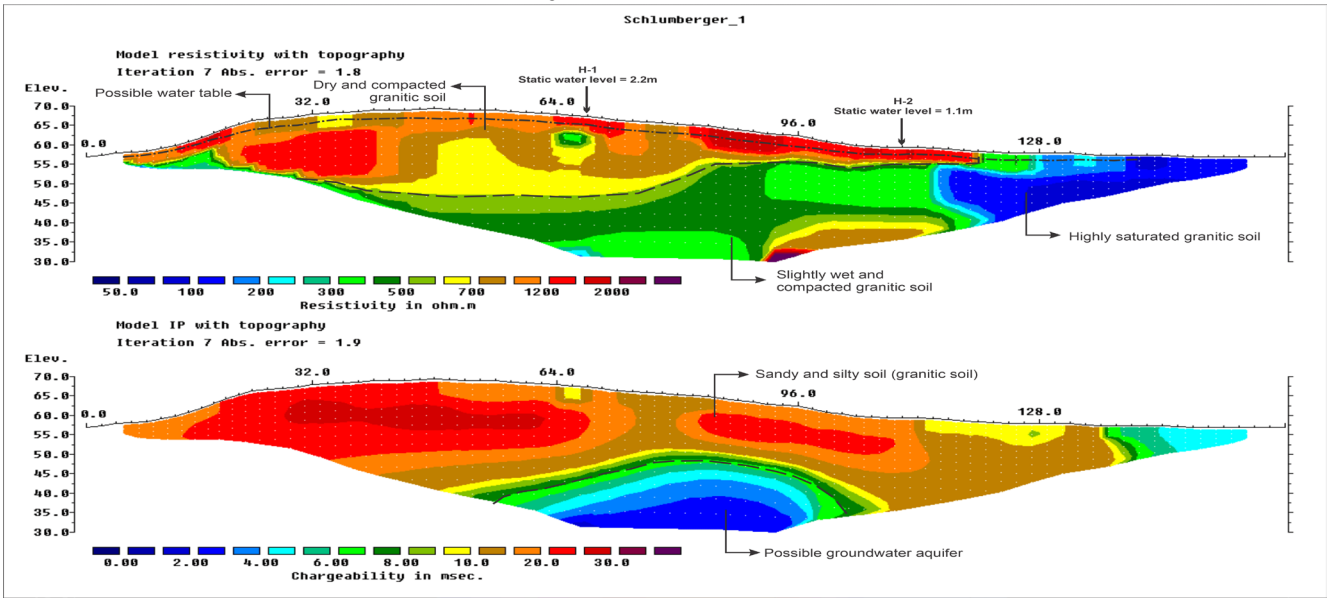

Figure 3: 2D Inverted Resistivity and Chargeability Tomograms for Survey Line 1 at the study area

.4.2 Line 2: subsurface characteristics

The electrical profiles from Line 2 (Figure 4) traverse a slightly higher elevation on the central part of the hill, and the shallow subsurface exhibits conditions similar to those observed along Line 1. Resistivity within the 0–5 m depth range remains high (500–2000 Ω·m), indicating a dry and compacted near-surface soil. Chargeability values across this shallow horizon are consistently low to moderate, generally below 10 milliseconds, and correspond to sandy–silty granitic regolith. Toward the flanks of the line, however, the sections reveal broad zones of significantly reduced resistivity (50–200 Ω·m) extending to greater depths. These coincide with deeper chargeability responses above 10 milliseconds, forming an apparent anomaly between approximately 60 and 100 m along the profile. The co-occurrence of low resistivity and enhanced chargeability is diagnostic of highly weathered, clay-enriched material that has been infiltrated by groundwater, most plausibly linked to lateral recharge from river infiltration. This feature is therefore interpreted as a substantial groundwater-bearing aquifer horizon within the weathered granitic mass.

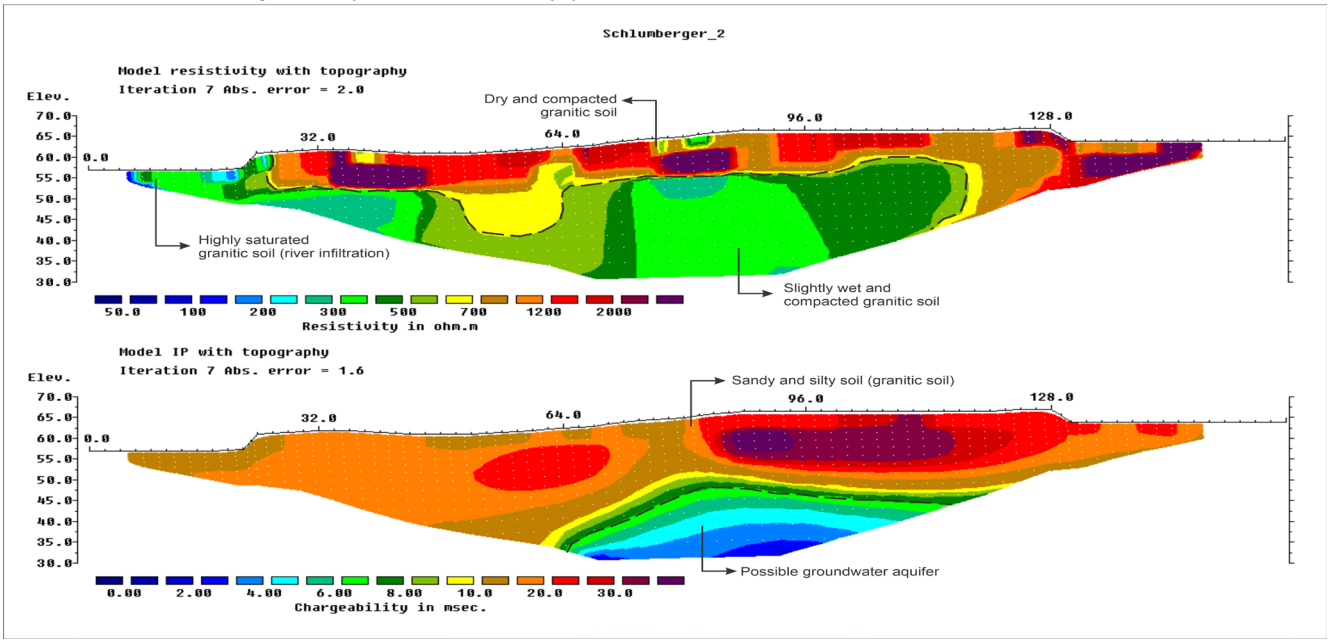

Figure 4: 2D Inverted Resistivity and Chargeability Tomograms for Survey Line 2 at the study area.

4.3 Line 3: subsurface characteristics

The geophysical section for Line 3 (Figure 5) again shows clear stratification between near-surface and deeper subsurface domains. In the upper 5 m, resistivity varies between 200 and >2000 Ω·m, reflecting a mix of dry, compacted granitic soil and slightly moist compacted soil horizons. Chargeability values in this shallow layer remain uniformly low to moderate (0–10 milliseconds), consistent with a regolith dominated by silty to sandy textures and only minor clay alteration. Below this shallow interval, a much larger low-resistivity body (50–200 Ω·m) becomes evident, extending laterally from a horizontal distance of 40 to 90 m and vertically below an elevation of 55 m. Within the same zone, chargeability increases markedly to values exceeding 10 milliseconds, forming a broad anomaly that aligns with the low resistivity feature. Such a combined response is interpreted as a thick, highly weathered, and clay-rich zone that is strongly water-saturated, consistent with previous studies that applied ERT/IP in clay-rich aquifers, contaminant monitoring, and REE exploration (Chambers et al., 2014; Uhlemann et al., 2017; Ogungbade et al., 2021), representing one of the most promising aquifer-like bodies observed in the study area. These findings parallel other forensic geophysical analyses in highly weathered terrains, such as slope failures in the Lesser Himalaya, where integrated methods revealed similar subsurface conditions (KC et al., 2025).

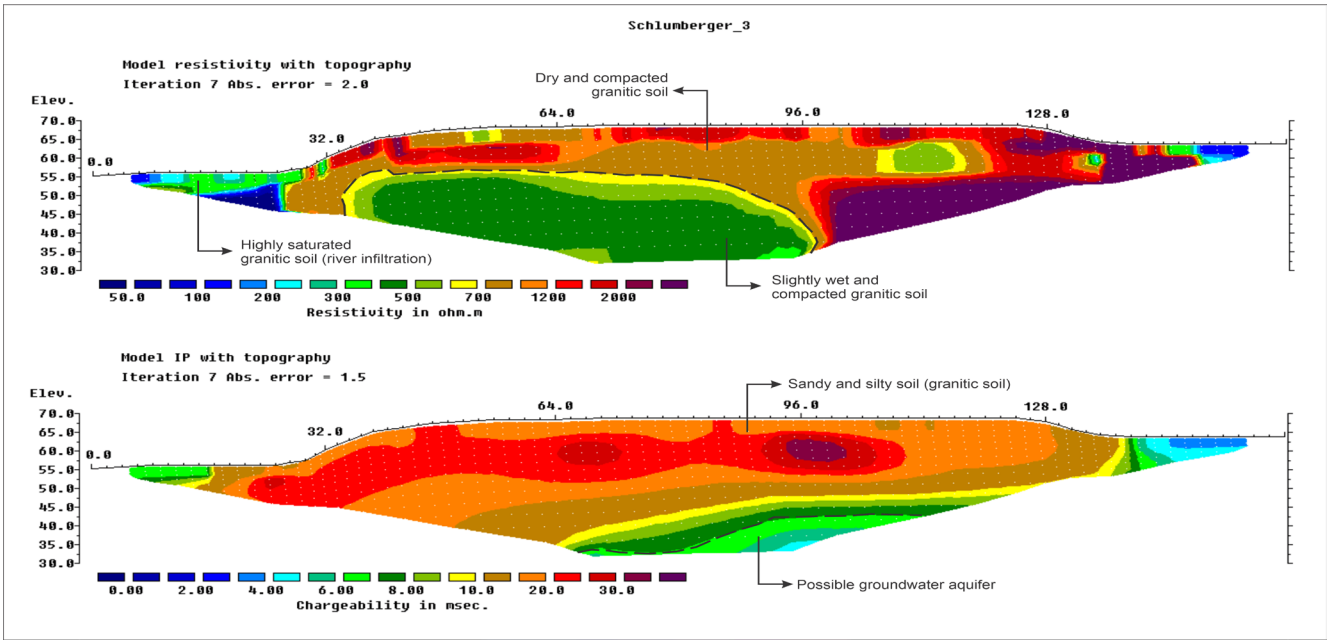

Figure 5: 2D Inverted Resistivity and Chargeability Tomograms for Survey Line 3 at the study area.

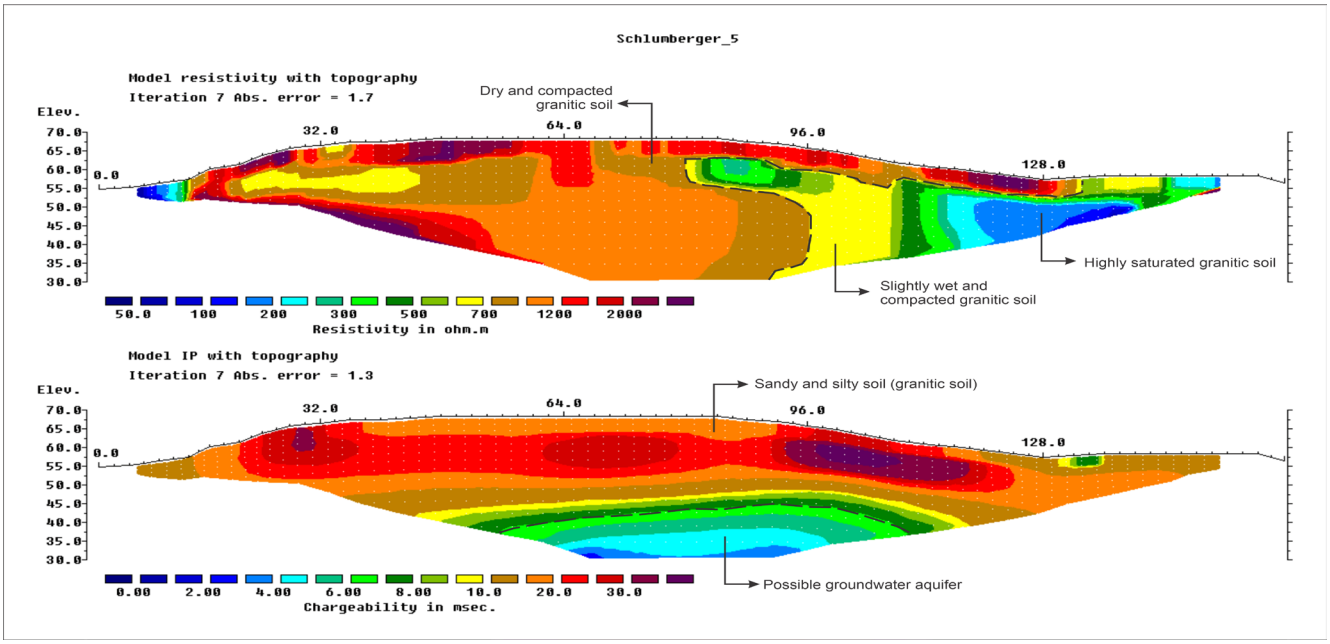

Figure 6: 2D Inverted Resistivity and Chargeability Tomograms for Survey Line 4 at the study area.

4.4 Line 4: subsurface characteristics

The tomograms for Line 4 (Figure 6) reveal shallow resistivity values in the range of 200 to more than 2000 Ω·m within the 0–5 m interval, suggesting dry to slightly wet compacted granitic soil. The chargeability in this shallow horizon remains consistently low to moderate (0–10 milliseconds), further supporting the interpretation of sandy to silty regolith with limited clay development. A significant departure from this shallow trend occurs toward the eastern end of the profile, where a broad zone of reduced resistivity (50–200 Ω·m) extends from near the surface to deeper levels. Within this zone, a localized chargeability anomaly with values exceeding 10 milliseconds is present. The overlap of low resistivity and elevated chargeability in this sector indicates the presence of a saturated, clay-enriched weathered body, which can be confidently interpreted as a potential groundwater-bearing horizon embedded within the decomposed granitic substratum.

The integrated interpretation of the ERI and IP results provides a robust and comprehensive understanding of the subsurface lithological distribution, weathering patterns, and inferred structural features within the metaigneous terrains of UMK Jeli. The consistent correlation between specific resistivity and chargeability signatures across all four profiles enables the development of a conceptual model that elucidates the complex interplay between geology, weathering, and hydrogeology in this tropical environment.

4.5 Delineation of Lithological Units and Weathering Profiles

The integration of resistivity and chargeability data across all four survey lines provides a clear distinction between fresh to slightly weathered bedrock and the more deeply weathered, clay-enriched zones. Fresh to intact metaigneous bedrock is characterized by consistently high resistivity values, often greater than 700–1000 Ω·m, and correspondingly low to moderate chargeability responses, typically ranging from approximately 4 to 8 milliseconds. These electrical properties reflect a compact, relatively unfractured rock mass with limited porosity and minimal clay alteration. Such zones typically appear at depth or within elevated portions of the profiles, where weathering intensity is reduced. Intermediate resistivity values in the range of 200–700 Ω·m are more indicative of moderately weathered material such as compacted granitic soil or saprolite. Although this material retains elements of its original rock fabric, it has undergone notable chemical alteration, which increases porosity and promotes the formation of secondary minerals, particularly clays. Chargeability responses in these horizons generally remain within the low to moderate range (<10 milliseconds), aligning with the presence of sandy to silty soils with minor clay components.

By contrast, the most significant features in the tomograms are the low-resistivity anomalies (50–200 Ω·m) that consistently coincide with elevated chargeability values exceeding 10 milliseconds. These anomalies are observed across all profiles but are most pronounced in several key locations: (i) the western sector of Line 1, where a thick zone of highly saturated granitic soil is linked to a possible shallow aquifer; (ii) the central portion of Line 2, where river infiltration appears to recharge a deeply weathered body; (iii) the broad anomaly along Line 3 between 40 and 90 m horizontal distance, which defines one of the thickest saturated weathered zones encountered; and (iv) the eastern end of Line 4, where low resistivity and high chargeability converge within a large weathered body. These low-resistivity/high-chargeability zones are diagnostic of clay-rich saprolitic layers that are both water-saturated and structurally weakened. Comparable multidisciplinary approaches, integrating geophysics with geomorphology and hydrogeological observations, have also been applied to deep-seated coastal landslides in Europe (Girard et al., 2020). In tropical granitic terrains, such horizons represent the most favorable settings for REE enrichment because weathering processes tend to leach REEs from primary minerals and concentrate them within the secondary clay matrix. Consequently, the identified zones in this study constitute priority targets for further exploration, including drilling and geochemical sampling, to evaluate their mineral potential.

5. CONCLUSION

This investigation, which integrated ERI and IP techniques, successfully characterized the complex subsurface architecture of the metaigneous terrain at Jeli. The results consistently distinguished between the shallow regolith and deeper weathered horizons. In the near-surface zone (0–5 m depth), resistivity values remained high, while chargeability responses were restricted to low to moderate levels (0–10 msec). These signatures confirm the presence of relatively dry, compacted granitic soil with limited clay content, in agreement with the examiner's observation that shallow layers exhibit low chargeability. At greater depths, however, distinct anomalies emerged where low resistivity (50–200 Ω·m) coincided with elevated chargeability (>10 msec). These features, repeatedly identified across all four profiles, represent zones of intense weathering and clay enrichment, commonly saturated by groundwater. Such zones are of particular significance because tropical weathering processes in granitic terrains often mobilize and re-concentrate Rare

Earth Elements (REEs) into secondary clay minerals. The delineation of these deeper clay-rich horizons therefore provides a robust geophysical basis for prioritizing REE exploration targets. Overall, the combined ERI and IP survey not only clarified the distribution of fresh bedrock, moderately weathered layers, and deeply weathered saturated zones but also underscored the importance of separating shallow low-chargeability horizons from deeper high-chargeability anomalies during interpretation. By integrating ERI and IP with surface geological observations, a comprehensive model of the subsurface was developed, in line with established applications of geophysics in environmental, engineering, and mineral exploration studies (Telford et al., 1990; Soupios et al., 2007) that enhances the predictive framework for REE exploration in Jeli and similar tropical metaigneous settings.

ACKNOWLEDGEMENT

We extend our appreciation to Universiti Malaysia Kelantan for providing the necessary instruments and resources for this research. The GREAT Technopreneurship Centre funded this work under grant no. R/GRT/A1300/01684A/008/2021/0096. Additionally, we appreciate the contributions of the staff and students of the Department of Geosciences and the Department of Biotechnology and Engineering. We sincerely appreciate the help of anonymous reviewers, whose suggestions and criticisms significantly improved the work.

REFERENCES

Abidin, H. Z., Hendrasto, E., & Sidiq, T. P. (2015). Application of electrical resistivity tomography for groundwater exploration in volcanic terrain, Indonesia. Environmental Earth Sciences, 74(1), 499–512. https://doi.org/10.1007/s12665-015-4046-8

Adeniran, M. A., Oladunjoye, M. A., & Doro, K. O. (2024). Assessing the use of electrical resistivity for monitoring crude oil contaminant distribution in unsaturated coastal sands under varying salinity. Geosciences, 14(11), 308. https://doi.org/10.3390/geosciences14110308

Alam, J., & Dick, P. (2024). Induced polarization of clay-rich materials. 4. Water content and temperature effects in bentonites. Geophysics, 90(1), 1–69. https://doi.org/10.1190/geo2022-0500.1

Badavath, N., & Sahoo, S. (2025). Geospatial assessment and mapping landslide susceptibility for the Garo Hills Division, Meghalaya, India. Geological Journal, 1–18. https://doi.org/10.1002/gj.5269

Briški, M., Stroj, A., Kosović, I., & Borović, S. (2020). Characterization of aquifers in metamorphic rocks by combined use of electrical resistivity tomography and monitoring of spring hydrodynamics. Geosciences, 10(4), 137. https://doi.org/10.3390/geosciences10040137

Binley, A., & Kemna, A. (2005). DC resistivity and induced polarization methods. In Rubin & Hubbard (Eds.), Hydrogeophysics. Springer.

Chambers, J. E., Wilkinson, P. B., Uhlemann, S., Sorensen, J. P. R., Roberts, C., Newell, A. J., Ward, W. O. C., Binley, A., & Williams, P. J. (2014). Derivation of lowland groundwater vulnerability from geoelectrical imaging. Journal of Contaminant Hydrology, 162–163, 27–42. https://doi.org/10.1016/j.jconhyd.2014.03.003

Dahlin, T., & Zhou, B. (2004). A numerical comparison of 2D resistivity imaging with 10 electrode arrays. Geophysical Prospecting, 52(5), 379–398. https://doi.org/10.1111/j.1365-2478.2004.00423.x

Dahlin, T. (2001). The development of DC resistivity imaging techniques. Computers & Geosciences, 27(9), 1019–1029. https://doi.org/10.1016/S0098-3004(00)00160-6

Fox, R. C. (1979). Topographic effects in resistivity and induced-polarization surveys. Geophysics, 45(1), 75–93. https://doi.org/10.1190/1.1440957

Girard, G., Grandjean, G., Thiery, Y., Maquaire, O., François, B., Lissak, C., & Costa, S. (2020). Hydrogeological assessment of a deep-seated coastal landslide based on a multi-disciplinary approach. Geomorphology, 354, 107440. https://doi.org/10.1016/j.geomorph.2020.107440

Hussain, Y., Campos, J. E. G., Borges, W. R., Uagoda, R. E. S., Hamza, O., & Havenith, H.-B. (2022). Hydrogeophysical characterization of fractured aquifers for groundwater exploration in the Federal District of Brazil. Applied Sciences, 12(5), 2509. https://doi.org/10.3390/app12052509

Ismail, N. I., & Yaacob, W. W. W. (2018). Application of electrical resistivity tomography (ERT) for slope failure investigation: A case study from Kuala Lumpur. Jurnal Teknologi (Sciences & Engineering), 80(5). https://doi.org/10.11113/jt.v80.11624

KC, R., Adhikari, K., Maharjan, K., Ojha, B., Niraula, U., & Timalsina, S. (2025). Forensic investigation of roadside cut slope landslide in the Lesser Himalayan region of Nepal. Natural Hazards, 121(8), 9757–9776. https://doi.org/10.1007/s11069-025-07208-0

Loke, M. H., & Barker, R. D. (1996). Rapid least-squares inversion of apparent resistivity pseudosections by a quasi-Newton method. Geophysical Prospecting, 44(1), 131–152. https://doi.org/10.1111/j.1365-2478.1996.tb00142.x

Luo, Q., Sun, W., Chen, R., Mi, X., & Yao, H. (2025). A magnetotelluric signal acquisition and monitoring system based on a cloud platform. Applied Sciences, 15(10), 5598. https://doi.org/10.3390/app15105598

Martorana, R., & Capizzi, P. (2023). Evaluation of artifacts and misinterpretation in 2D electrical resistivity tomography caused by three-dimensional resistive structures of regular or irregular shapes. Applied Sciences, 13(3), 2015. https://doi.org/10.3390/app13032015

Metwaly, M., El-Qady, G., & Al-Garni, M. (2012). Subsurface characterization in tropical regions using resistivity and induced polarization techniques. Arabian Journal of Geosciences, 5(6), 1225–1234. https://doi.org/10.1007/s12517-011-0302-6

Ogungbade, A. M., Adeoye, J. A., & Oladunjoye, M. A. (2021). Geoelectrical and geochemical approaches for rare earth element exploration in weathered granites. Journal of African Earth Sciences, 180, 104226. https://doi.org/10.1016/j.jafrearsci.2021.104226

Perrone, A., Lapenna, V., & Piscitelli, S. (2014). Electrical resistivity tomography technique for landslide investigation: A review. Engineering Geology, 183, 31–42. https://doi.org/10.1016/j.enggeo.2014.09.009

Rusydy, I., Fathani, T. F., Al-Huda, N., Sugiarto, S., Iqbal, K., Jamaluddin, K., & Meilianda, E. (2021). Integrated approach in studying rock and soil slope stability in a tropical and active tectonic country. Environmental Earth Sciences, 80(2), 58. https://doi.org/10.1007/s12665-020-09357-w

Satir, T., El Hatib, A. A., & Akca, I. (2021). Electrical resistivity tomography for seawater intrusion mapping in coastal aquifers: A case study from Turkey. Water, 13(2), 267. https://doi.org/10.3390/w13020267

Sulaiman, N., Ariffin, N., Sulaiman, M., & Jamil, R. (2022). Groundwater exploration using electrical resistivity imaging (ERI) at Kemahang, Tanah Merah, Kelantan. IOP Conference Series: Earth and Environmental Science, 1102(1), 012027. https://doi.org/10.1088/1755-1315/1102/1/012027

Soupios, P., Kouli, M., Vallianatos, F., Vafidis, A., & Stavroulakis, G. (2007). Application of integrated methods in groundwater investigations: ERT, IP, and hydrogeological data. Journal of Applied Geophysics, 62(3), 266–281. https://doi.org/10.1016/j.jappgeo.2006.12.003

Tandon, R., Gupta, V., Venkateshwarlu, B., & Joshi, P. (2022). An assessment of Dungale landslide using remotely piloted aircraft system (RPAS), ground penetration radar (GPR), and Slide & RS2 softwares. Natural Hazards, 113(2), 1017–1042. https://doi.org/10.1007/s11069-022-05334-7

Telford, W. M., Geldart, L. P., & Sheriff, R. E. (1990). Applied Geophysics (2nd ed.). Cambridge University Press. https://doi.org/10.1017/CBO9781139167932

Uhlemann, S., Chambers, J. E., Wilkinson, P. B., Maurer, H., Merritt, A., Gunn, D. A., Meldrum, P. I., & Kuras, O. (2017). Four-dimensional imaging of moisture dynamics during landslide reactivation. Earth Surface Processes and Landforms, 42(14), 2253–2270. https://doi.org/10.1002/esp.4163

Vann, S., Puttiwongrak, A., Suteerasak, T., & Koedsin, W. (2020). Delineation of seawater intrusion using geo-electrical survey in a coastal aquifer of Kamala Beach, Phuket, Thailand. Water, 12(2), 506. https://doi.org/10.3390/w12020506

Zaid, H. A. H., Arifin, M. H., Kayode, J. S., Basori, M. B. I., Umor, M. R., & Hazim, S. H. (2023). Application of 2-D electrical resistivity imaging and induced polarization methods for delineating gold mineralization at Felda. Sains Malaysiana, 52(2), 305–320. https://doi.org/10.17576/jsm-2023-5201-25

